Experimental Mechanics (2010) 50:125–133
DOI 10.1007/s11340-008-9213-6

Detwinning of High-Purity Zirconium: *In-Situ* Neutron Diffraction Experiments

G. Proust · G.C. Kaschner · I.J. Beyerlein · B. Clausen · D.W. Brown · R.J. McCabe · C.N. Tomé

Received: 18 May 2008 / Accepted: 1 December 2008 / Published online: 25 December 2008

Abstract Twinning is an important deformation mode in hexagonal metals to accommodate deformation along the *c*-axis. It differs from slip in that it accommodates shear by means of crystallographic reorientation of domains within the grain. Such reorientation has been shown to be reversible (detwinning) in magnesium alloy aggregates. In this paper we perform *in-situ* neutron diffraction reversal experiments on high-purity Zr at room temperature and liquid nitrogen temperature, and follow the evolution of twin fraction. The experiments were motivated by previous studies done on clock-rolled Zr, subjected to deformation history changes (direction and temperature), in the quasi-static regime, for temperatures ranging from 76 K to 450 K. We demonstrate here for the first time that detwinning of $\{10\bar{1}2\}\langle 10\bar{1}1\rangle$ tensile twins is favored over the activation of a different twin variant in grains of high-purity polycrystalline Zr. A visco-plastic self-consistent (VPSC) model developed previously, which includes combined slip and twin deformation, was used here to simulate the reversal behavior of the material and to interpret the experimental results in terms of slip and twinning activities.

Keywords Neutron diffraction · Zirconium · Twinning · Texture · Plasticity

G. Proust · G.C. Kaschner · I.J. Beyerlein · B. Clausen · D.W. Brown · R.J. McCabe · C.N. Tomé
Los Alamos National Laboratory,
Los Alamos, NM 87545, USA

G.C. Kaschner
e-mail: kaschner@lanl.gov

I.J. Beyerlein
e-mail: irene@lanl.gov

B. Clausen
e-mail: clausen@lanl.gov

D.W. Brown
e-mail: dbrown@lanl.gov

R.J. McCabe
e-mail: rmccabe@lanl.gov

C.N. Tomé
e-mail: tome@lanl.gov

G. Proust (✉)
School of Civil Engineering Australian Key Centre for Microscopy & Microanalysis,
University of Sydney,
Sydney, NSW 2006, Australia
e-mail: g.proust@usyd.edu.au

Introduction

The work presented here is part of a general study to characterize and model the mechanical behavior of different hexagonal close-packed (hcp) metals over a wide range of temperatures under monotonic, strain-path change or temperature change loadings. One of these materials is high-purity zirconium with an interstitial impurity level lower than 100 ppm. Zirconium exhibits several slip and twinning modes to accommodate deformation due to its hcp crystallographic structure. The diversity of the deformation mechanisms explains the highly anisotropic mechanical behavior displayed by this material. The activation of one specific mode depends on composition, crystallographic orientation, loading direction, temperature and strain rate. Various studies have been realized to understand the effect of these parameters on the activation of the deformation modes, for example see references [1–6].

This particular material was clock-rolled and then annealed at 550°C for an hour, which results in a microstructure of equiaxed twin-free grains of 20–25 μm average grain size and a strongly in-plane basal texture: the majority of the grains are oriented such that their *c*-axis is almost aligned with the through-thickness direction of the plate [see Fig. 1(a)]. Figure 1(b) shows some of the previously obtained stress–strain curves at different temperatures and at a strain rate of 10^{-3} s^{-1} [6]. The occurrence of

the different deformation mechanisms during these tests has been characterized experimentally [5, 7] and by using a visco-plastic self-consistent (VPSC) model [8–10]. From these experiments, we were able to draw the following observations regarding twinning:

1) at room temperature, during in-plane tension (IPT), there is no twinning activity;
2) during in-plane compression (IPC), $\{10\bar{1}2\}\langle 10\bar{1}\bar{1}\rangle$ tensile twinning was observed for temperatures ranging from 76 to 450 K; the twin fraction increases with decreasing temperature at a given strain;
3) during through-thickness compression (TTC), $\{11\bar{2}2\}\langle 11\bar{2}\bar{3}\rangle$ compressive twinning was observed for temperatures ranging from 76 to 150 K. For temperatures above room temperature no compressive twins were observed.

In parallel to the Zr study, work has been carried out to characterize and model the mechanical behavior of magnesium alloy AZ31. Detwinning is an additional deformation mechanism that has been observed in AZ31 during strain-path change deformation [11] and also during *in-situ* neutron diffraction reversal experiments realized at the Manual Lujan Jr., Neutron Scattering Center, LANSCE, Los Alamos National Laboratory [12]. The crystal deformation process of detwinning is similar to re-twinning, although nucleation is not required [13]. Detwinning is activated within the primary twins, and reorients the twin domain back to its original orientation. According to experiments realized on various hcp metals, the stress required for detwinning is less than that for twin nucleation, but greater than that for twin growth [14]. To verify if such mechanism occurs also in high-purity Zr, we have designed a set of *in-situ* neutron diffraction experiments that were realized at LANSCE and the results obtained during these experiments are described and analyzed in the rest of the paper. We also used our VPSC model [10] to predict and interpret the reversal experiments; the results of these simulations are presented in the last section of the paper.

As mentioned earlier, different twinning modes can be activated during the deformation of Zr, but here we focus our attention on $\{10\bar{1}2\}\langle 10\bar{1}\bar{1}\rangle$ tensile twins and we want to study its behavior during reversal loading. We know from our previous work on this material that tensile twins $\{10\bar{1}2\}\langle 10\bar{1}\bar{1}\rangle$ appear over a wider temperature range than the other twin types, and that secondary twinning activity inside them is not prevalent at low strains [8]. Therefore, if detwinning occurs in Zr, it is more likely to happen, and easier to characterize, for this particular twinning mode. Moreover, this particular tensile twinning mode changes the texture of the material drastically by reorienting the twinned domains of the grains by 86.6°, which facilitates detection using neutron diffraction as we will explain in the experimental results section.

Experimental Set-Up

Neutron diffraction is a well suited technique to obtain bulk measurements in Zr and was previously used to

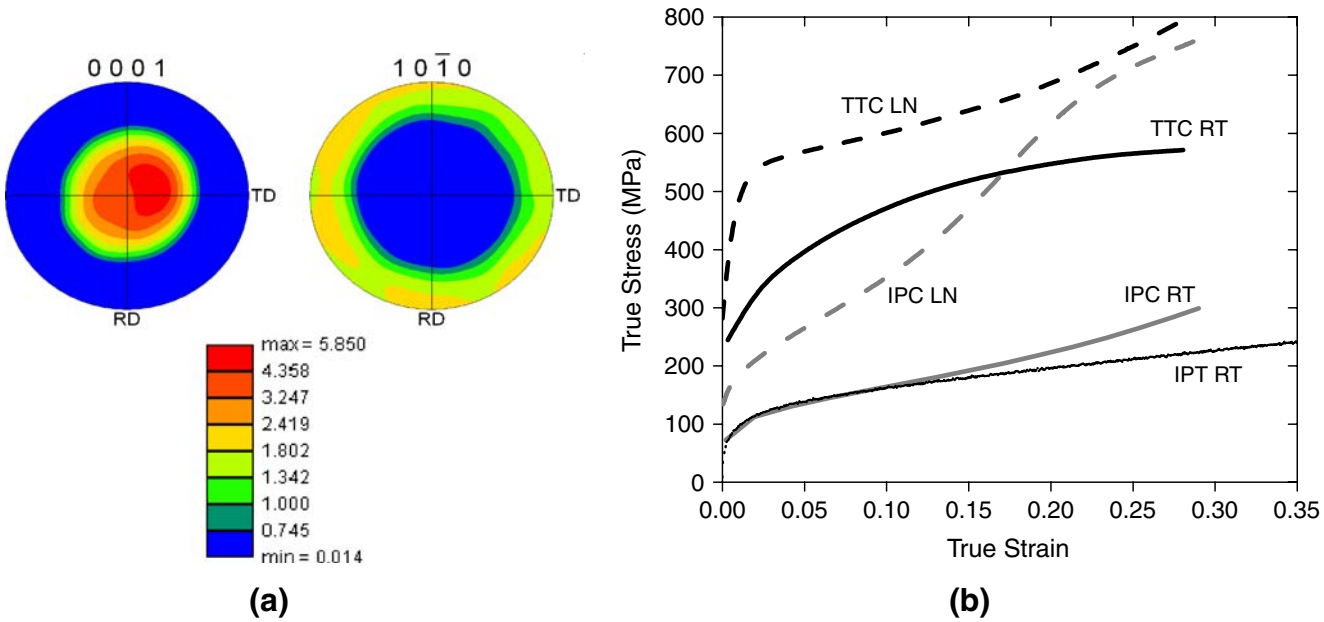

Fig. 1 (**a**) Initial texture of the high-purity Zr studied; (**b**) mechanical behavior of the Zr studied at room temperature (*RT*) and liquid nitrogen (*LN*) temperature when deformed in through-thickness compression (*TTC*), in-plane compression (*IPC*) and in-plane tension (*IPT*)

measure the texture of deformed Zr specimens and to characterize the volume fraction of $\{11\bar{2}2\}\langle 11\bar{2}3\rangle$ compressive twinning [15]. During deformation, twinning takes place throughout the entire sample and the full penetration of the specimens by neutrons provides reliable volumetric measurements. Neutron diffraction measurements were performed during *in-situ* uniaxial deformation on the Spectrometer for Materials Research at Temperature and Stress (SMARTS) at LANSCE. Details of the technique are published elsewhere [16] and only a short description is given here. Figure 2 shows a schematic of the neutron diffraction instrument and the orientation of the applied load in relation to the beam [17]. A horizontal load frame was used to load the samples in tension and compression with the load axis at 45° from the incident beam. Detectors on either side of the specimen simultaneously record data with diffraction vectors, parallel (longitudinal) $Q_{\parallel}$ (−90°) and transverse $Q_{\perp}$ (+90°), to the applied load [17, 18].

The specimens were designed according to ASTM standard E606-92. However, the final dimensions retained were dictated by the thickness of the clock-rolled Zr plate. The maximum thickness at the grips was 9.5 mm (corresponding to the thickness of the plate) and the rest of the dimensions were adapted to this maximal thickness. Figure 3 shows the orientation of the specimens with respect to the Zr plate. The experiments were designed to have the direction 3 of the plate parallel to the $Q_{\perp}$ direction and the direction IP2 parallel to the $Q_{\parallel}$ direction. Each experiment is divided in four segments. The load direction is fixed along IP1. First the sample is subjected to a compressive load that activates twinning (segment 1). The sample is then unloaded (segment 2) and subjected to a tensile load (segment 3). The last segment (segment 4) consists in unloading the sample. Two experiments have been run on high-purity Zr samples:

1. Segments 1 to 4 are realized at room temperature.
2. Segments 1 and 2 are realized at liquid nitrogen temperature and segments 3 and 4 at room temperature.

As the compression phase of the second experiment is realized at liquid nitrogen temperature, more twins will be introduced in the material. However, as the sample is immersed in a liquid nitrogen bath to maintain the correct temperature, it is not possible to take texture measurements during the compression phase of the experiment because liquid nitrogen scatters the neutrons. The tensile phase of this experiment is realized at room temperature and *in-situ* neutron diffraction measurements are possible in this case. By performing the experiments at two different temperatures, we can monitor the effect of temperature on the detwinning mechanism.

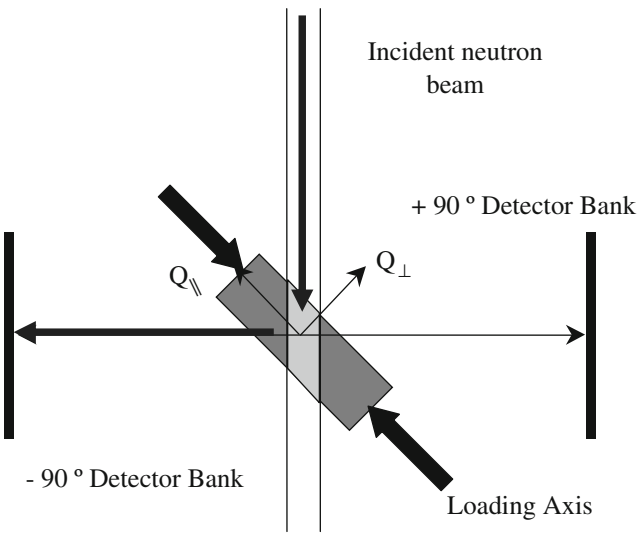

Fig. 2 Schematic of the neutron diffraction instrument

Experimental Results

The diffraction geometry of SMARTS coupled with the as-rolled texture of Zr is advantageous for the study of this particular tensile twinning. Initially, diffracted intensity from the basal (0002) poles is weak (almost totally absent) in the $Q_{\parallel}$ detector [Fig. 4(b)] and strong in the $Q_{\perp}$ detector [Fig. 4(a)]. On the opposite, prismatic pole $(10\bar{1}0)$ intensity is initially strong in the $Q_{\parallel}$ detector [Fig. 4(b)] and weak (almost totally absent) in the $Q_{\perp}$ detector [Fig. 4(a)]. As mentioned earlier, tensile twins $\{10\bar{1}2\}\langle 10\bar{1}\bar{1}\rangle$ reorient regions in the grains by 86.6°. Given the sample orientation, this nearly 90° reorientation results in a transfer of part of (0002) diffraction intensity from the $Q_{\perp}$ to the $Q_{\parallel}$ detector, while part of the prismatic plane diffraction intensity transfers from the $Q_{\parallel}$ to the $Q_{\perp}$ detector. This is experimentally observed and shown in Fig. 4(c) and (d) after 8% IPC of the sample at room temperature. In Fig. 4(c), we see that the prismatic $(10\bar{1}0)$ peak that was initially almost non-existent is now present in the diffraction pattern. Similarly, in Fig. 4(d), we see that the almost non-existent basal pole (0002) peak is now present. Following the evolution of the intensities of these poles respectively to each other allows the detection of even small amounts of twins in the material. In this particular example, even though only 5% of the material has twinned, the twins can be detected by analyzing these neutron diffraction patterns.

Experiment 1

The first sample was deformed entirely at room temperature, first in compression to a strain of 8% (which is the

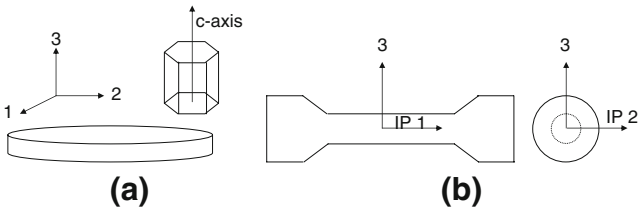

Fig. 3 (**a**) Schematic representation of the crystallographic orientation in the initial plate; (**b**) reversal test specimen, IP1 and IP2 are two in-plane directions. In both pictures, the *c*-axis of the crystals is oriented parallel to the direction 3 of the original plate. The loading direction is fixed in IP1 for all tests

maximum deformation possible with this sample geometry before buckling of the specimen occurs) and then in tension to a strain of 8% as well. The stress–strain curve obtained is shown in Fig. 5(a). The serrations on the curves reflect stress relaxation taking place during each of the neutron diffraction measurements. The compression curve is similar to the IPC curve from the macroscopic sample shown in Fig. 1(b). At 8% strain a twinning signature on the stress–strain curve (rapid increase in the hardening rate that can be observed in Fig 1(b) for TTC and IPC at liquid nitrogen and IPC at room temperature) is not yet noticeable. However, from our previous macroscopic experiments realized at room temperature, we measured by electron backscatter diffraction (EBSD) a 7% twin fraction at 10% strain [see Fig. 7(a)], and from this we estimate that about 5% twin fraction is introduced in the material at 8% strain. Therefore like in the initial IPC phase, the volume fraction associated with any potential detwinning of these twins during the subsequent IPT phase will also not be sufficient to show a twinning signature in the stress–strain curve.

However, information can be retrieved from the variation of intensities of the various peaks representing the prismatic

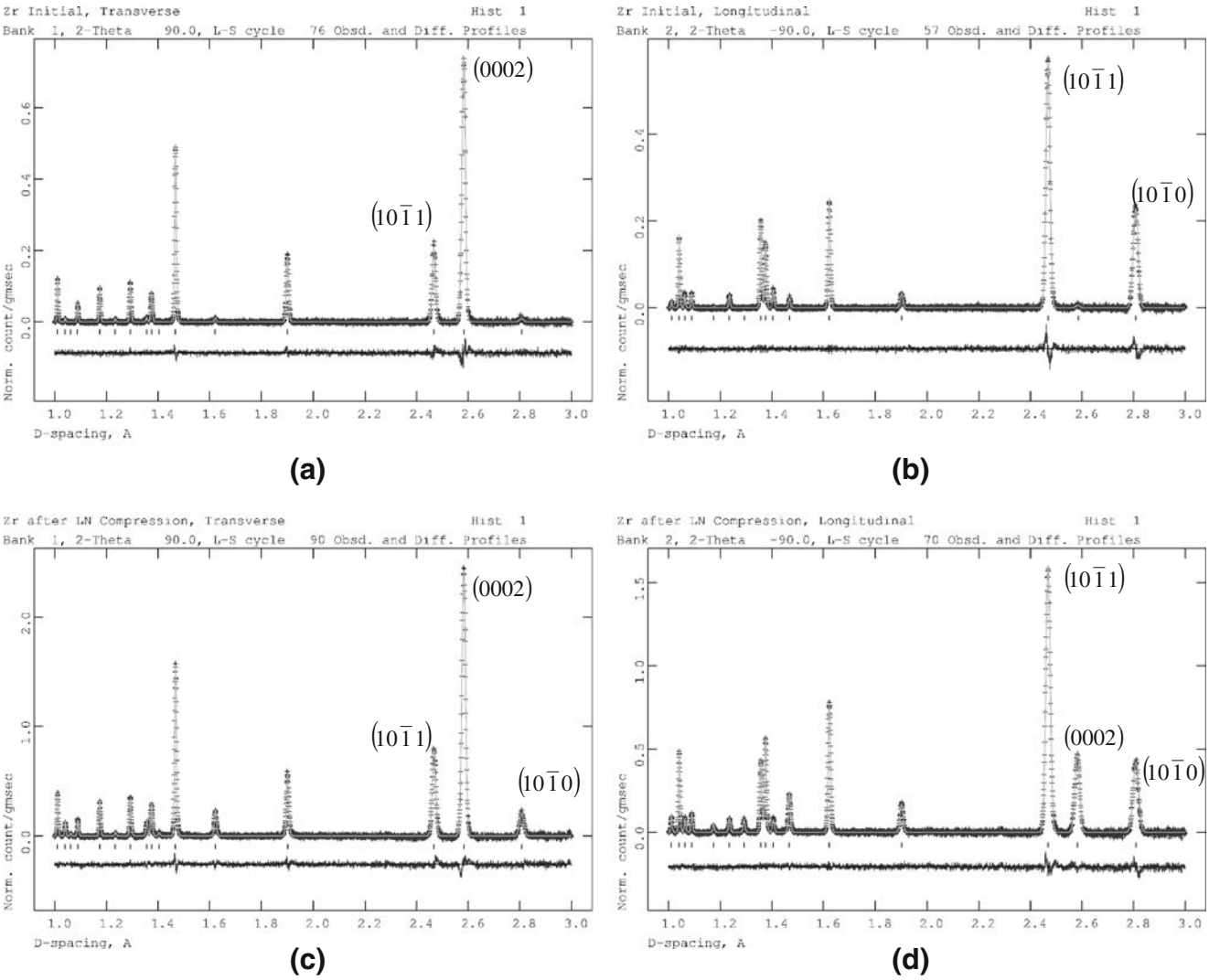

Fig. 4 Diffraction patterns obtained before the test started in (**a**) transverse and (**b**) longitudinal detector banks and after 8% IPC at room temperature in (**c**) transverse and (**d**) longitudinal detector banks. The position of the peaks corresponding to the poles of interest is indicated on each diffraction pattern

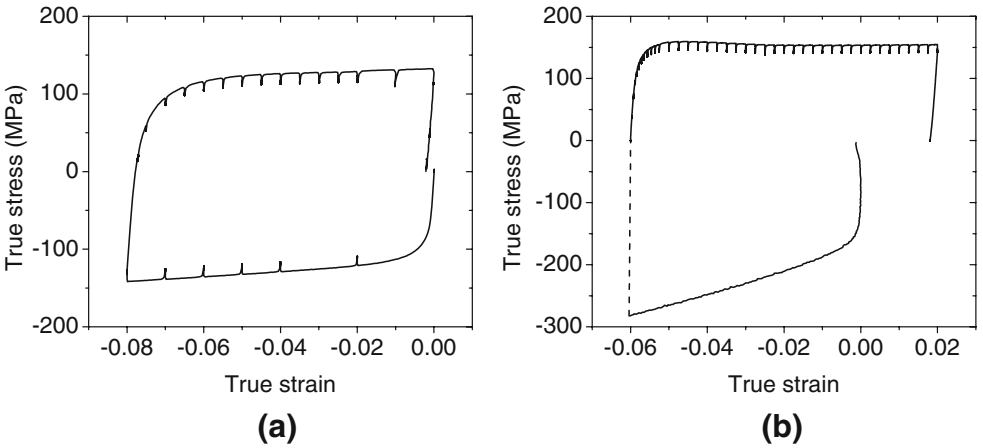

Fig. 5 True stress–true strain curves obtained during (**a**) room temperature and (**b**) liquid nitrogen-room temperature reversal experiments. In (**b**) the liquid nitrogen temperature compression stress–strain curve comes from previous macroscopic experiments. The irregularities in the curves are caused by the tests being stopped for the neutron diffraction measurements

and basal planes. Here we only use the $10\bar{1}0$ and 0002 peaks because the changes in intensities are strongest for these two. The other peaks also show changes, but with a smaller variation. The variation with strain of the normalized values of the intensity for the peaks representing the (0002) and the $(10\bar{1}0)$ poles measured for each detector bank is given in Fig. 6(a). At the start of the experiments, most grains are oriented such that their c-axes are parallel to the $Q_{\perp}$ direction so there is a high intensity for the (0002) pole in this particular detector bank (the curve on the graph is labeled 0002_Trans) while the intensity for that particular pole is lower in the other detector bank (the curve on the graph is labeled 0002_Long). On the other hand, the prismatic poles $(10\bar{1}0)$ of the grains are parallel to the $Q_{\parallel}$ direction so there is a high intensity for the $(10\bar{1}0)$ pole in that particular detector bank (the curve on the graph is labeled $10\bar{1}0$_Long) while the intensity for this particular pole is lower in the other detector bank (the curve on the graph is labeled $10\bar{1}0$_Trans). While the experiment is running, the intensity of each curve varies. For the 0002_Trans curve corresponding to the (0002) poles measured by the transversal detector bank, the lower points correspond to the measurement done during the compression phase of the experiment (For each curve, the lower points correspond to the compressive phase of the experiment, while the upper points were measured during the tensile phase of the experiments.) We notice that the intensity decreases as the compressive strain increases, because twinning reorients the *c*-axis in grain domains, and aligns them with the compression direction. Similarly, we notice a decrease in the intensity in the $10\bar{1}0$_Long curve corresponding to the $(10\bar{1}0)$ poles measured in the longitudinal detector bank. On the other hand, we see that the other two curves, the $10\bar{1}0$_Trans curve representing the $(10\bar{1}0)$ poles measured by the transversal detector bank and the 0002_Long curve representing the (0002) poles measured by the longitudinal detector bank, show an increase in intensity. Even if the changes in peak intensities are small they are proof of the drastic crystallographic reorientation of some grain domains. These twinned domains now have their *c*-axis contained in the plane of the plate (perpendicular to their original position). Such a reorientation cannot

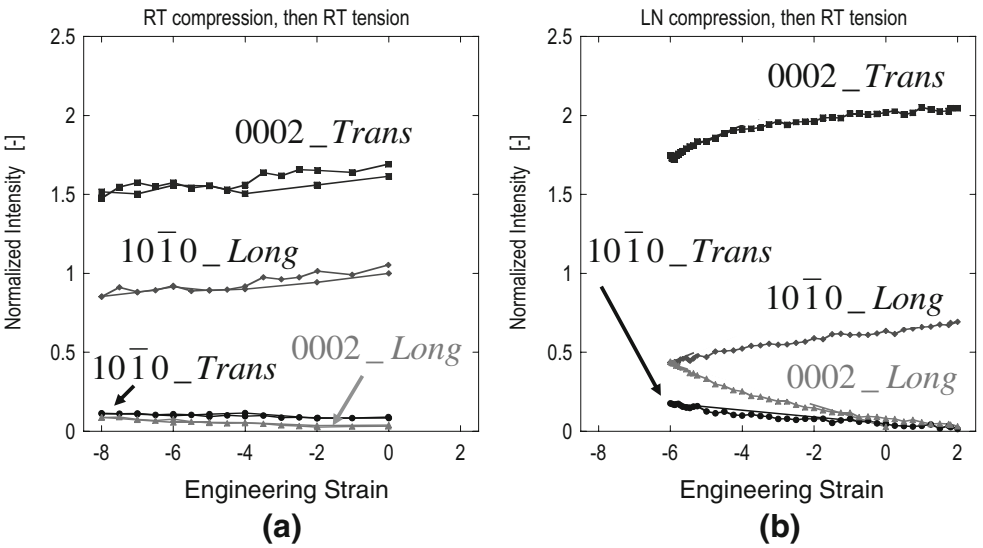

Fig. 6 Normalized $(10\bar{1}0)$ and (0002) peak intensities collected from the transverse detector bank (*_Trans*) and the longitudinal detector bank (*_Long*) during (**a**) room temperature and (**b**) liquid nitrogen-room temperature reversal experiments (measurements were made only during the tensile segment of the experiment). The normalization has been done using the initial values of the intensity of each peak as reference

be explained by slip at such low strains. Instead, we know that $\{10\bar{1}2\}\langle 10\bar{1}\bar{1}\rangle$ tensile twinning reorients the *c*-axis at 86.6° from its original position, and explains the change in the peak intensity observed.

During the tensile phase of the experiment, we can observe that the variation of the peak intensities is reversed and, after 8% strain, the peaks show the same intensities as they had before the sample was subjected to deformation. This drastic change in crystal orientation can only be explained, this time again, by reversal twinning (detwinning) of the grain domains that had previously twinned. As the intensities come back exactly to where they were initially, the grains have the same orientation as initially. The twin orientations have disappeared from the diffraction patterns. Therefore detwinning is taking place in the Zr aggregate.

Experiment 2

The second experiment was similar to the first one except for the temperature of the compressive segment. The sample was first subjected to a compressive load to a strain of 6% and then unloaded at liquid nitrogen temperature. At this temperature, we know that more twins are introduced in the material [7]. Afterwards, the sample was loaded in tension at room temperature to a strain of 8%. The bath surrounding the specimen prevented us from taking neutron diffraction and strain measurements during the compression phase of the test. During the tensile phase of the experiment, realized at room temperature, it was possible to take *in-situ* measurements and they are shown in Fig. 6(b). The compressive stress–strain curve shown in Fig. 5(b) corresponds to a separate mechanical test done at liquid nitrogen temperature. The stress–strain curve obtained during the *in-situ* tensile phase of the experiment is also shown in Fig. 5(b). The twinning signature is also absent from this curve and, as before, additional data needs to be analyzed to determine whether detwinning has occurred. The amount of strain introduced in the sample during the compression phase of the experiment is approximately 6% and was obtained by measuring the change in sample length. Using the previous macroscopic data obtained at liquid nitrogen [7], we can estimate the

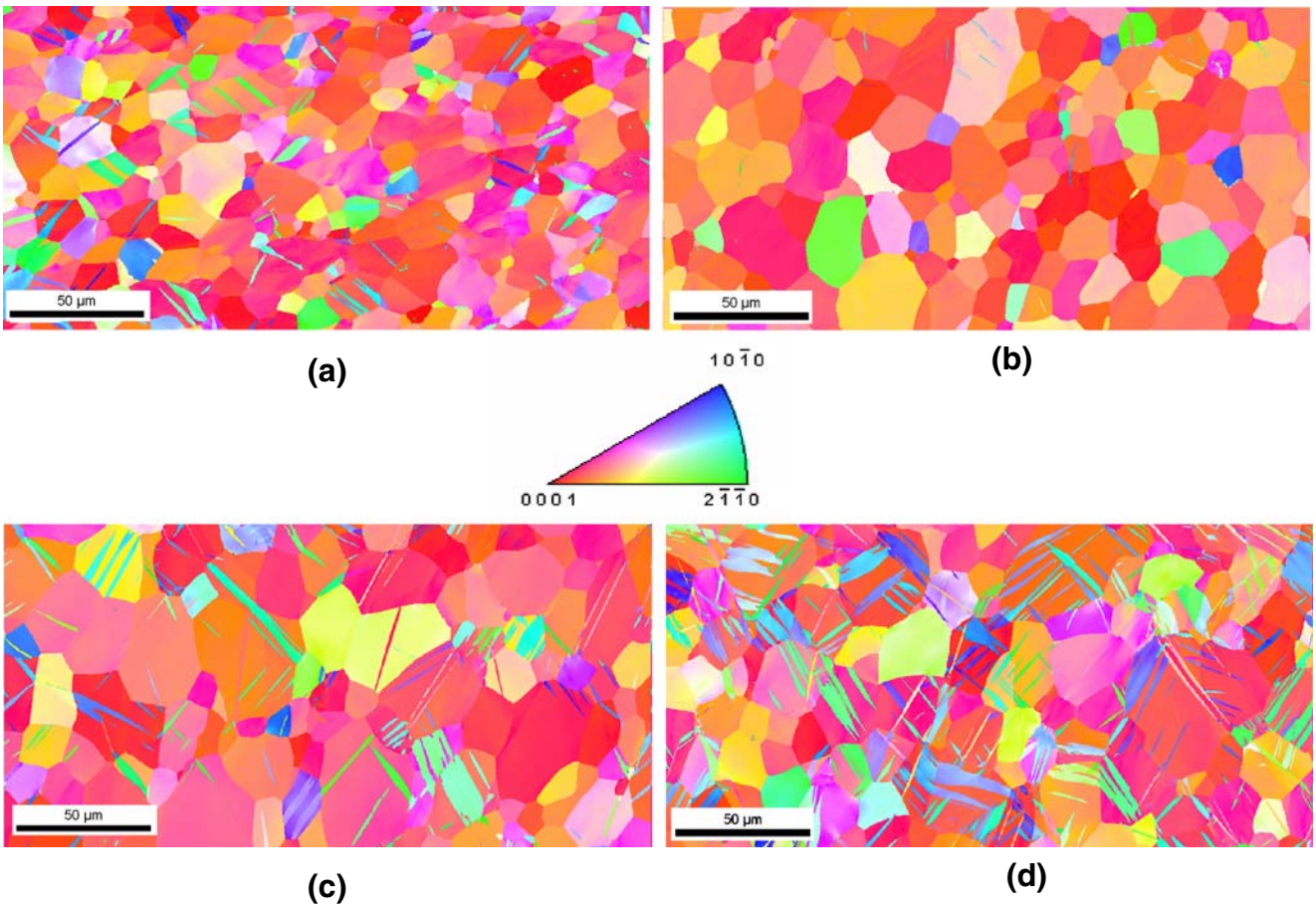

Fig. 7 001 inverse pole figure map of (**a**) macroscopic sample deformed by IPC to a strain of 10% at room temperature; (**b**) reversal test specimen subjected to compression at liquid nitrogen temperature followed by tension at room temperature, (**c**) macroscopic sample deformed by IPC to a strain of 4.2% at liquid nitrogen temperature; and (**d**) macroscopic sample deformed by IPC to a strain of 8.9% at liquid nitrogen temperature. Each color represents a crystallographic orientation

amount of twinning introduced in the aggregate to be approximately 8%.

We can analyze the evolution of the peak intensities observed during the tensile phase of the test, shown in Fig. 6(b). During the tension phase of the experiment, we observe an increase in the fraction of orientations having their *c*-axis parallel to direction 3 of the initial plate, which indicates a reversal towards the initial orientation distribution. To verify that detwinning is actually happening we run an EBSD scan on the sample after it had been subjected to the compression–tension cycle. The result of this scan is shown in the inverse pole figure (IPF) map in Fig. 7(b). In that figure we see very thin twins left inside a few grains, but most grains are actually twin-free. We can compare this microstructure with the microstructures of Zr samples deformed macroscopically to 4.2% and 8.9% strain by IPC at liquid nitrogen shown on Figs. 7(c) and (d), respectively. If detwinning had not occurred during the reversal experiment, the microstructure should be similar to the microstructures of the samples deformed to 4.2% and 8.9%, which is not what we observe. Therefore, the only explanation to this almost twin-free microstructure is that the twins introduced during compression have disappeared during the tension phase of the experiment.

Predictions

Predictions of plastic deformation and relative activities of each slip and twinning mode are obtained using our VPSC code with the predominant twin reorientation (PTR) scheme to account for twinning effect on texture evolution. A Voce law is used to incorporate the influence of twinning on hardening of the material during deformation. Details of the model and the Voce hardening parameters used in these simulations can be found elsewhere [10]. In the PTR scheme the whole grain is reoriented by twinning when a volume threshold is met. We incorporate the idea of detwinning in this model by allowing individual orientations (grains) to reorient by twinning more than once, although we acknowledge that this is a rather crude way of accounting for detwinning. Although the model allows for four deformation mechanisms, prismatic <a> slip, pyramidal <c+a> slip, $\{11\bar{2}2\}\langle 11\bar{2}3\rangle$ compressive twinning and $\{10\bar{1}2\}\langle 10\bar{1}1\rangle$ tensile twinning, to accommodate the predicted deformation, the dominant deformation mechanisms in IPC and IPT are prismatic slip and $\{10\bar{1}2\}\langle 10\bar{1}\bar{1}\rangle$ tensile twinning. Figure 8(a) compares the experimental and simulated curves for the experiment run at liquid nitrogen temperature and then room temperature. Because our model does not take into account the Bauschinger effect, the predicted reload curve (the IPT curve) overestimates the hardening rate. Still, the calculated flow stresses are not far from the experiment. It is more interesting to look at the mode activity predictions shown on Fig. 8(b), where the *x*-axis corresponds to accumulated strain regardless of the loading direction. During the compressive phase of the test, prismatic slip and tensile twinning accommodate the deformation. But upon reloading in tension, we see that the deformation is again accommodated by prismatic slip and tensile twinning. The latter is a consequence of having pre-strained the material in IPC; the model predicts only prismatic slip and no twinning activity when the material is loaded monotonically in IPT (see ref. [10]). Moreover, in the model, the twinning taking place in the reload occurred within the twinned orientations generated in the preload. In the second twinning event, the twin system variant that is activated was found to be the same variant that twinned during preload. However instead of operating in the matrix, it operates in the reoriented twin domain. As further confirmation, the twin volume fractions predicted by our model at liquid nitrogen temperature during the IPC and IPT match well with the measurements. The effective twin fraction predicted by our model after 6% IPC at liquid nitrogen temperature is 11% (The hardening parameters were not fitted to match the experimentally measured twin volume fraction.) More interestingly, the models predicted that when the material is further deformed by 6% IPT, 4%

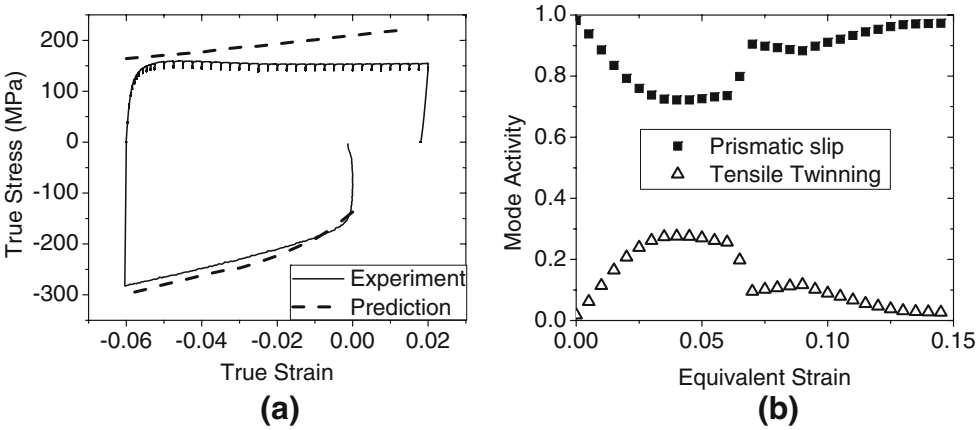

Fig. 8 (**a**) Comparison of the experimental and predicted stress–strain curve for the case where the IPC is realized at liquid nitrogen temperature and the IPT at room temperature; (**b**) prediction of the deformation modes that are active during deformation. The equivalent strain (Von Mises) is independent of the direction of loading

of the material detwins and after 8% IPT, 9% of the material detwins. So almost all the original 11% twins introduced during IPC at liquid nitrogen temperature detwins by 8% IPT at room temperature. To summarize, our model predicts that the twins that were created during IPC are twinned again during IPT and that the same twin variant as the one that created the original twin domain is activated inside that twin domain. This mechanism can be assimilated to detwinning from a crystallographic point of view.

Conclusions

These two experiments prove that detwinning occurs also in high-purity Zr. Moreover, we have shown that even if twins are introduced at a low temperature where twinning is more prevalent, nearly full detwinning is accomplished upon reversal even at a higher temperature where twinning is generally less prevalent. There are two possible explanations. (1) Temperature is not a factor in the twin variant choice and only crystallographic orientation influences twin selection. In our temperature range, tensile twinning will be preferred over pyramidal <c+a> slip when the *c*-axis is in tension and, as a consequence, tensile twinning will be activated in the twin during the reversal stroke. (2) Detwinning is easier to activate than twinning, and the material would "prefer" to detwin than to activate another twin variant inside the primary twin. Since twinning first requires a nucleation stage before propagation, and nucleation is believed to require higher stresses than propagation, detwinning will be favored because it does not require the nucleation phase.

Our complementary modeling effort provides insight into detwinning in pure Zr. Our model does not predict twinning activity during monotonic IPT, but it predicts that twinning activity will occur after twins have been introduced in the material during IPC prestraining. The model also confirms that detwinning, rather than secondary twinning is the favored mechanism upon reversal. Moreover, we see a good correlation between the measured and predicted twin volume fractions during IPC followed by IPT.

More accurate models still need to be developed. The current model uses a simple twin reorientation scheme (PTR), yet a more sophisticated composite grain model for twin reorientation has been developed recently [8]. A first attempt was made in [19] to incorporate detwinning in the case of magnesium using the composite grain model. In both [19] and in the present work, the onset of twinning was controlled by critical resolved shear stresses described by an empirical Voce law, an approach which limits the predictive capability of these models. The characterization of detwinning presented here will certainly aid in developing a more physically based model for twin nucleation, growth, and detwinning. Along with this effort, further experimental evidence is necessary to better understand the detwinning mechanism.

Acknowledgments Work at LANL was supported under Office of Basic Energy Sciences Project FWP 06SCPE401 and U.S. DOE Contract No. W-7405-ENG-36.

References

1. Pochettino AA, Gannio N, Vial Edwards C et al (1992) Texture and pyramidal slip in Ti, Zr and their alloys. Scr Metall Mater 27:1859–1863. doi:10.1016/0956-716X(92)90033-B.
2. Bingert JF, Mason TA, Kaschner GC et al (2002) Deformation twinning in polycrystalline Zr: insights from electron backscattered diffraction characterization. Metall Mater Trans A 33A:955–963.
3. Fundenberger JJ, Philippe MJ, Esling C (1990) Mechanical twinning at high temperatures in some hexagonal alloys. Scr Metall Mater 24:1215–1220. doi:10.1016/0956-716X(90)90330-J.
4. Kaschner GC, Gray GT III (2000) The influence of crystallographic texture and interstitial impurities on the mechanical behavior of Zirconium. Metall Mater Trans A 31A:1997–2003. doi:10.1007/s11661-000-0227-7.
5. McCabe RJ, Cerreta EK, Misra A et al (2006) Effects of texture, temperature and strain on the deformation modes of zirconium. Philos Mag 8623:3595–3611. doi:10.1080/14786430600684500.
6. Kaschner GC, Bingert JF, Liu C et al (2001) Mechanical response of zirconium—II. Experimental and finite element analysis of bent beams. Acta Mater 49:3097–3108. doi:10.1016/S1359-6454(01)00191-4.
7. McCabe RJ, Proust G, Cerreta EK et al (2008) Quantitative analysis of deformation twinning in zirconium. Int J Plast. doi:10.1016/j.iplas.2008.03.010.
8. Proust G, Tomé CN, Kaschner GC (2007) Modeling texture, twinning and hardening evolution during deformation of hexagonal materials. Acta Mater 55:2137–2148. doi:10.1016/j.actamat.2006.11.017.
9. Beyerlein IJ, Tomé CN (2008) A dislocation-based constitutive law for pure Zr including temperature effects. Int J Plast 24:867–895. doi:10.1016/j.ijplas.2007.07.017.
10. Kaschner GC, Tome CN, Beyerlein IJ et al (2006) Role of twinning in the hardening response of zirconium during temperature reloads. Acta Mater 54:2887–2896. doi:10.1016/j.actamat.2006.02.036.
11. Jain A, Agnew SR (2006) Effect of twinning on the mechanical behavior of a magnesium alloy sheet during strain path changes. In: Luo AA, Neelameggham N, Beals R (eds) Magnesium technology. TMS, Warrendale, PA, p 219.
12. Brown DW, Jain A, Agnew SR et al (2007) Twinning and detwinning during cyclic deformation of Mg alloy AZ31B. Mater Sci Forum 539–5434:3407.
13. Lou XY, Li M, Boger RK et al (2007) Hardening evolution of AZ31B Mg sheet. Int J Plast 231:44. doi:10.1016/j.ijplas.2006.03.005.
14. Partridge PG (1965) Cyclic twinning in fatigued hexagonal close-packed metals. Philos Mag 12:1043–1054. doi:10.1080/14786436508228133.
15. Rangaswamy P, Bourke MAM, Brown DW et al (2002) A study of twinning in zirconium using neutron diffraction and polycrystalline modeling. Metall Mater Trans A 33A:757–763.
16. Bourke MAM, Dunand D, Ustundag E (2002) SMARTS—a spectrometer for strain measurement in engineering materials. Appl Phys A A74:S1707. doi:10.1007/s003390201747.

17. Brown DW, Agnew SR, Bourke MAM et al (2005) Internal strain and texture evolution during deformation twinning in magnesium. Mater Sci Eng A 3991–2:1. doi:10.1016/j.msea.2005.02.016.
18. Bourke MAM, Goldstone JA, Holden TM (1992) Residual stress measurement using the pulsed neutron source at LANSCE. In: Hutchings, MT, Krawitz, AD (eds) Measurement of residual and applied stress using neutron diffraction. Kluwer, The Netherlands, pp 369–382.
19. Proust G, Tomé CN, Jain A et al (2008) Modeling the effect of twinning and detwinning during strain-path changes of magnesium alloy AZ31. Int J Plast. doi:10.1016/j.iplas.2008.05.005.